



The Potential Role of Bone Marrow Derived Mesenchymal Stem Cells Conditioned Medium in the Suppression of Hepatocellular Carcinoma In Vitro: Modulation of Apoptosis

Mahmoud Abdelhady Metwally^{1*}, Mona Abdelftah Ali¹, Farouk Abdelmohdy¹, Mohamed Kassab¹, Tarek Kamal Abouzed² and Khalil Fathy Abou-Easa¹

¹Department of Cytology and Histology, Faculty of Veterinary Medicine, Kafrelsheikh University, Kafrelsheikh, Egypt

²Department of Biochemistry, Faculty of Veterinary Medicine, Kafrelsheikh University, Kafrelsheikh, Egypt.

ABSTRACT

Bone marrow mesenchymal stem cells (BMMSCs) can home to cancerous cells and suppress their growth. However, few studies have investigated the impact of conditioned medium harvested from BMMSCs on carcinogenesis. This study investigated the effect of BMMSCs-conditioned medium (BMMSCs-CM) on the hepatoma cell line HepG2 and described the underlying molecular mechanisms involved. We isolated BMMSCs and identified them using flowcytometry and culture characteristics, then prepared BMMSCs-CM. HepG2 cells were treated with various concentrations of BMMSCs-CM for up to 72 h. The methylthiazolyldiphenyl-tetrazolium (MTT) assay showed decreased proliferation, while flowcytometry showed increased apoptosis and cell cycle arrest in the G0/G1 phase with inhibition of entry into the S phase. RT-PCR showed *p53* upregulation and *Bcl-2* downregulation in mRNA expression. Moreover, Western blotting and flowcytometry revealed elevated *p53* and lowered *Bcl-2* protein levels. In addition, ELISA findings showed decreased toll-like receptor 4 (TLR4) concentration. Taken together, our findings highlight the potent therapeutic function of BMMSCs-CM in suppressing HepG2 cancerous cells across multiple platforms, including proliferation, apoptosis, cell cycle, and oncogene expression. Furthermore, our findings suggest that the Notch and TLR4/NF- κ B signaling pathways may be targets of BMMSCs-CM for tumor cell suppression.

Article Information

Received 16 March 2022

Revised 25 April 2022

Accepted 11 May 2022

Available online 08 September 2022 (early access)

Authors' Contribution

MAM provided the concept of the research, performed the experiments and wrote the manuscript. MAA and FA supervised the study. MK helped in manuscript writing. TKA assisted in the data analysis in the experiment. KFA supervised the study and helped in the lab work.

Key words

Bone marrow-derived Mesenchymal stem cells, Mesenchymal stem cells conditioned medium, Hepatocellular carcinoma, HepG2 cell apoptosis, Liver cancer

INTRODUCTION

Liver cancer persists as a global health issue as its prevalence is increasing worldwide (Craig *et al.*, 2020; Llovet *et al.*, 2021). It is anticipated that more than 1 million people will be diagnosed with liver cancer each year by 2025 (Llovet *et al.*, 2021). The most frequent type of liver cancer is hepatocellular carcinoma (HCC), which accounts for 90% of all liver cancer cases globally (Craig *et al.*, 2020). Among Egyptians, HCC is ranked as the fourth most common form of cancer (Rashed *et al.*, 2020). Moreover, HCC is the world's fourth most common cause of cancer mortality (Yang *et al.*, 2019).

There are multiple major risk factors for inducing HCC, including hepatitis C virus (HCV), hepatitis B virus (HBV), non-alcoholic liver disease, consumption of food contaminated with aflatoxin B1 and excessive alcohol intake (Abdelkawy *et al.*, 2020).

HCC develops as a consequence of an imbalance between excessive cell proliferation and apoptosis, which is primarily mediated by the tumor suppressor gene *p53* and the anti-apoptotic gene *Bcl-2*. Declined levels of *p53* and elevated levels of *Bcl-2* have been linked to hepatocarcinogenesis and have been extensively described in HCC (Mahfouz *et al.*, 2021; Mansour *et al.*, 2021).

Surgery, radiation, and chemotherapy are all traditional cancer treatments that are either invasive or produce unfavorable side effects. Therefore, finding innovative approaches to slow the course of HCC and to prevent metastasis is critical (Mohamed *et al.*, 2019; Selim *et al.*, 2019).

Advancements in stem cell biology have facilitated real-world clinical applications of cell therapy and tissue regeneration (Kwon *et al.*, 2018). Stem cells, particularly mesenchymal stem cells (MSCs), have shown unique biological properties such as self-renewal, multilineage

* Corresponding author: mahmoud_abdelhady@vet.kfs.edu.eg
0030-9923/2022/0001-0001 \$ 9.00/0



Copyright 2022 by the authors. Licensee Zoological Society of Pakistan.

This article is an open access article distributed under the terms and conditions of the Creative Commons Attribution (CC BY) license (<https://creativecommons.org/licenses/by/4.0/>).

differentiation, and immunomodulation, leading to their widespread use in regenerative medicine (Tae *et al.*, 2006).

MSCs are adult, nonhemopoietic, multipotent cells that can differentiate into various types of cells and can be isolated from numerous sources in the body, including umbilical cord (Erices *et al.*, 2000), adipose tissue (Zuk *et al.*, 2002), placenta (Fukuchi *et al.*, 2004), peripheral blood (Villaron *et al.*, 2004) and bone marrow (El-Magd *et al.*, 2019). Bone marrow mesenchymal stem cells (BMMSCs) can be harvested with ease from a simple bone marrow aspirate, making them a simple and attractive source for acquiring MSCs.

Many studies have been conducted to clarify the interactions between MSCs and cancer cells; however, the precise roles that MSCs play in cancer modulation is debatable. On one hand, MSCs have been shown to exhibit protumor effects and promote metastasis in human breast cancer via chemokine secretion (Karnoub *et al.*, 2007). On the contrary, using MSCs in a kaposi sarcoma model produced strong pro-apoptotic and antitumorigenic effects (Khakoo *et al.*, 2006), and in a glioblastoma multiforme model caused disturbances in tumor cells' growth and proliferation pathways with selective induction of cancer cell apoptosis (Akimoto *et al.*, 2013).

MSCs transplantation carries its own risks, whether it's infection or graft failure (Lukomska *et al.*, 2019), making the use of MSCs secretome such as exosomes (Alzahrani *et al.*, 2018; Zahran *et al.*, 2020), through the preparation of conditioned medium (CM) a valid option in mitigating transplantation associated complications (Di Santo *et al.*, 2009). Investigations regarding Adipose tissue-derived MSCs-CM have shown potent anti-tumor effects experimentally (Yang *et al.*, 2014). However, few studies have reported the influence of BMMSCs-CM on HCC.

This study aimed to investigate how BMMSCs-CM could affect carcinogenesis in an HCC cell line, HepG2, in vitro, through modulating cellular proliferation, apoptosis, and cancer marker expression.

MATERIALS AND METHODS

Chemicals and cell line

Dulbecco's modified Eagle's medium (DMEM) (Cat. no. 41965-039) and fetal bovine serum (Cat. no. 10270-106) were purchased from Gibco, USA. Penicillin-streptomycin (Cat. no. P4333), Amphotericin B (Cat. no. A2942), and RNase-free water (Cat. no. 7732-18-5) were bought from Sigma, USA. CyQUANT 3-[4, 5-dimethylthiazol-2-yl]-2, 5 diphenyl tetrazolium bromide (MTT) cell viability assay kit (Cat. no. V-13154), Maxima SYBR green (Cat. no. K0222), Pierce rapid gold BCA protein assay kit (Cat. no. A53225) and TMB blotting substrate solution (Cat. no. 34018) were obtained from Thermo Scientific, USA. Quanti Tects Reverse Transcription kit (Cat. no. 205310) was bought from Qiagen, USA. Annexin V-FITC stain kit (Cat. no. 556547), and the antibodies against CD44 (Cat. no. 550989), CD90 (Cat. no. 555595), CD34 (Cat. no. 348053), and CD105 (Cat. no. 561443) were acquired from BD Pharmingen, USA. The antibodies against *p53* (Cat. no. ab17990) (Cat. no. ab131442), *Bcl-2* (Cat. no. ab692) (Cat. no. ab196495), β -*actin* (Cat. no. ab8227), and HRP-conjugated secondary antibody (Cat. no. ab97185) were purchased from Abcam, UK. Human Toll-like receptor 4 (TLR4) ELISA Kit (Cat. no. ELH-TLR4) was bought from RayBiotech, USA. TRIzol reagent (Cat. no. 15596026) was acquired from Invitrogen, USA and the primers for *p53*, *Bcl-2*, and β -*actin* (Table I) were obtained from Integrated DNA Technologies (IDT)-Coralville, USA. HepG2 cells (human liver carcinoma cell line) was purchased from National Oncology Institute, Egypt.

Animals

Eight-week-old male albino rats from the Animal Center of Kafrelsheikh University weighing 90g were used for the isolation of BMMSCs-CM. Any operation involving the animals and their welfare followed the guidelines and was reviewed by the Research Ethics Committee of the Faculty of Veterinary Medicine, Kafrelsheikh University, giving the ethical approval.

Table I. The primers sequences for Real-Time PCR.

Gene	Nucleotide sequences	Reference
<i>P53</i>	F 5' CCTCAGCATCTTATCCGAGTGG 3' R 5' TGGATGGTGGTACAGTCAGAGC 3'	(Andries <i>et al.</i> , 2015)
<i>Bcl-2</i>	F 5' CATGTGTGTGGAGAGCGTCAAC 3' R 5' CAGATAGGCACCCAGGGTGAT 3'	(Baharara <i>et al.</i> , 2015)
β - <i>actin</i>	F 5' CCCGCCGCCAGCTCACCATGG 3' R 5' AAGTCTCAAACATGATCTGGGTC 3'	(Baharara <i>et al.</i> , 2015)

Isolation of bone marrow mesenchymal stem cells

The rats were sacrificed by cervical dislocation, and both the tibia and femur of both limbs were collected. The muscular and connective tissues covering the bones were detached and eliminated. The bones were further cleaned using sterile gauze to remove any residual tissue attached, and placed on an aseptic glass dish containing a mixture of DMEM and 10% FBS to conserve the tissue. A volume of 20 ml of maintenance medium was prepared in a test tube. Both ends of each bone were cut. Using a sterile 2 ml syringe, the maintenance medium in the tube was aspirated and forced slowly into the medullary cavity of each bone from one end. From the opposite end, the flushed content containing suspended bone marrow cells was received in a 15 ml Eppendorf tube, then centrifuged (Thermo Fisher Megafuge16R, USA) at 500g for 5 min. The supernatant was removed, and the bottom layer of suspended cells was pipetted into a 25-ml tissue culture flask previously filled with 4 ml of growth medium, consisting of DMEM, 10% FBS, and a 1% antimicrobial mixture of amphotericin B and penicillin-streptomycin. These flasks were incubated (Thermo Fisher Heracell 150i, USA) at 5% CO₂ and 37°C and passaged. The first and second passages took longer to adapt to in-vitro conditions, while the cells in the third passage required a relatively shorter time period to adapt to the new environment.

Identification of BMMSCs-CM

In the third passage, cells were identified according to the International Society for Cellular Therapy (ISCT) guidelines (Dominici *et al.*, 2006). The cells were evaluated for their fibroblast-like appearance and plastic adherence in culture (Dominici *et al.*, 2006). In addition, flowcytometry was used to determine the expression of CD44, CD90, and CD105, which are characteristic surface markers for BMMSCs (Dominici *et al.*, 2006; Secunda *et al.*, 2015), and CD34, which is an endothelial and hemopoietic surface marker (Secunda *et al.*, 2015). The flowcytometry procedure was performed according to the manufacturer's instructions, where 100 µl of cell suspension was prepared from third passage cells, using TRIS EDTA buffer. Cells were washed with PBS then centrifuged at 2000 rpm for 5 min. The supernatant was discarded, and the produced pellet was resuspended in 100 µl PBS. 7µl of FITC-anti-CD44 antibody, FITC-anti-CD90 antibody, FITC-anti-CD105 antibody, and FITC-anti-CD34 antibody were added separately, mixed well, and incubated at room temperature in the dark for 30 min. The cells were then washed with PBS, centrifuged, resuspended, and fixed in 200 µl 4% paraformaldehyde-PBS until flowcytometry.

Preparation of BMMSCs-CM

Identified BMMSCs from passage three were cultured in 75 ml culture flasks. A serum-free medium made up of DMEM and 10% FBS was used for culture, and flasks were incubated at 5% CO₂ and 37°C. After 24 h, the CM was collected, filtered through a 0.22 µm-diameter filter, and centrifuged at 1500g for 10 min, then preserved at -80°C until used.

Determination of cytotoxicity by MTT assay

Harvested BMMSCs-CM was used to treat HepG2 cells at different concentrations: 20%, 40%, 60%, 80%, and 100% which were prepared by diluting the CM using DMEM, each over the course of 24, 48, and 72 h. HepG2 cells grown in DMEM with 10% FBS were used as a negative control. The culture medium was changed every 24 h and the MTT cell viability assay was carried out according to the manufacturer's instructions. In brief, each test well received 10 µl of a previously prepared 12 mM MTT stock solution and was incubated at 37°C for 4 h. Next, 100 µl of previously prepared SDS-HCl was added to each test well and mixed thoroughly using a pipette, then incubated at 37°C in a humidified chamber for 4 h. Each sample was mixed again and the optical density was measured using a microplate reader (Biotek ELx800, USA) at 570nm. The inhibitory rate of BMMSCs-CM on the viability of HepG2 cells was analyzed using the following formula:

$$\text{Inhibitory Rate (\%)} = \left(1 - \frac{\text{OD570 value of experimental group}}{\text{OD570 value of control group}}\right) \times 100$$

Flowcytometry analysis of apoptosis and cell cycle

FITC Annexin V Apoptosis Detection Kit was used according to the manufacturer's instructions to assess the influence of BMMSCs-CM on HepG2 cell apoptosis. In brief, HepG2 cells cultured in DMEM and 10% FBS served as a negative control group, while another group of HepG2 cells was treated with 100% BMMSCs CM for 72 h. After treatment, at least 1×10⁶ of HepG2 cells were freshly harvested, washed twice with PBS and resuspended in binding buffer. The cells were then stained with Annexin V-FITC and incubated for at least 15 min in the dark. Following incubation, both the binding buffer and propidium iodide (PI) solutions were added. Finally, HepG2 cells were evaluated for apoptosis using flowcytometry (Biosciences BD Accuri C6 BD, USA). For cell cycle analysis, a cell suspension of 2×10⁶ treated HepG2 cells was prepared using ice cold PBS. The cells were then treated with 50 µl of a 100 µg/ml stock solution of RNase. 400 µl of a PI/Triton X-100 staining solution was added. Cells were incubated at 37°C for 15 min, and then data was acquired on a flow cytometer.

Real time polymerase chain reaction assay of p53 and Bcl-2

Total RNA was extracted from HepG2 cells treated with 100% BMMSCs CM for 72 h using TRIzol reagent according to the manufacturer's instructions. The RNA concentration was determined using a nanodrop spectrophotometer (Thermo Fisher Nanodrop 2000, USA) after dissolving the RNA pellet in RNase-free water. A Quanti Tects Reverse Transcription Kit was used to make cDNA from extracted RNA according to the manufacturer's instructions. In brief, 10 μ l of 2X RT reaction solution, 1 μ l of Quantiscript Reverse Transcriptase enzyme mix solution, and 1 μ g of RNA were combined with RNase-free water to make a total volume of 20 μ l. The mixture was incubated at 42°C for 15 min and at 95°C for 3 min. The RT-qPCR analysis was carried out using Maxima SYBR green and specific primer pairs of *p53*, *Bcl-2* and β -*actin* genes, with their sequences illustrated in Table I. β -*actin* served as the house-keeping gene. The thermal cycling was as follows: 95°C/10 min initial denaturation, followed by 45 cycles of 95°C/10 s, 60°C/15 s, and 72°C/15 s. The Rotor - Gene Q (Qiagen, USA) collected the data automatically and analyzed the value of the cycle threshold (Ct). The $2^{-\Delta\Delta C_t}$ method was used to analyze the relative quantitative data (Livak and Schmittgen, 2001).

Western blotting of p53 and Bcl-2

Whole-cell lysates were prepared from HepG2 cells that had been treated with 100% BMMSCs CM for 72 h. A BCA protein assay kit was used for measuring the protein concentration. Proteins (30 μ g) were loaded onto 12% sodium dodecyl sulfate–polyacrylamide slab gel for electrophoresis. Before immunodetection, electrolyzed proteins were transferred to a Hybond nylon membrane (GE Healthcare, USA), and then incubated overnight at 4°C with each of the following antibodies separately: anti-*p53* primary antibody (1:2000), anti-*Bcl-2* primary antibody (1:500), and anti β -*actin* primary antibody (1:1000). After washing the membrane in TBST, it was incubated at 37°C for 1hr in an appropriate HRP-conjugated secondary antibody (1:2000). The bands were observed by a 1-step TMB-blotting substrate solution. β -*actin* served as the house-keeping protein. TotalLab analysis software 1.0.1 was used to quantify the bands' optical density.

Flowcytometric analysis of p53 and Bcl-2

HepG2 cells treated with 100% BMMSCs CM for 72 h were analyzed using flowcytometry for the expression of *Bcl-2* and *p53* proteins. In brief, 100 μ l of cell suspension containing 10^6 cells/ml was prepared from treated HepG2 cells using TRIS EDTA buffer. Cells were washed with PBS then centrifuged at 2000 rpm for 5 min. The supernatant was discarded, and the produced pellet was resuspended

in 100 μ l PBS. 7 μ l of FITC-anti-*Bcl-2* antibody and FITC-anti-*p53* antibody were added separately, mixed well, and incubated at room temperature in the dark for 30 min. The cells were then washed with PBS, centrifuged, resuspended, and fixed in 200 μ l 4% paraformaldehyde-PBS until flowcytometry (Biosciences BD Accuri C6 BD, USA) analysis.

ELISA analysis of TLR4

The human TLR4 kit was used to determine changes in TLR4 concentration in HepG2 cells treated with 100% BMMSCs CM for 72 h. The procedure was carried out as directed by the manufacturer's instructions. The optical density was read immediately at 450nm using a microplate reader (Biotek ELx800, USA). The Intra-Assay CV%: <10%, and the Inter-Assay CV%: <12%. Further calculations were carried out according to the manufacturer's instructions and the TLR4 concentrations were determined.

Statistical analysis

One-way ANOVA and Student's t-test using GraphPad Prism 9.1.0 (GraphPad Software Inc., La Jolla, CA, USA) were used to determine the difference between the groups. Comparison of means was carried out with Dunnett's Multiple Comparison test. Data were presented as mean \pm standard deviation (SD), and significance was declared at $P < 0.05$.

RESULTS

Characterization of BMMSCs

BMMSCs harvested after the third passage of culture showed a positive capacity for plastic adherence. Microscopic evaluation revealed spindle, fibroblast like morphology with cytoplasmic processes extending in opposite directions. Furthermore, flowcytometric analysis revealed positive expression of BMMSCs specific markers CD44 (96.3%), CD90 (96.1%) and CD105 (98%), and negative expression of hemopoietic and endothelial marker CD34 (94.5%) (Fig. 1).

Effect of BMMSCs on HepG2 cell viability

To determine the effect of BMMSCs-CM on HepG2 cell viability, HepG2 cells were treated with 20%, 40%, 60%, 80%, and 100% BMMSCs-CM for 24, 48, and 72 h. The viability of HepG2 cells was determined using the MTT method. Results confirmed the presence of an inhibitory effect exerted by BMMSCs-CM on HepG2 cells. The inhibitory effect was elevated as the BMMSCs-CM concentration was increased and as the period of treatment was prolonged. All BMMSCs-CM groups (20%, 40%,

60%, 80%, and 100%) showed a significant inhibitory effect when compared to the control group, reaching as high as 48.23% at 100% BMMSCs-CM after 72 h of treatment, and as low as 16.89% at 20% BMMSCs-CM after 24 h of treatment (Fig. 2). Depending on the previous data, 100% BMMSCs-CM for 72h was the treatment of choice for further investigations; as it produced the highest cytotoxic effect on HepG2.

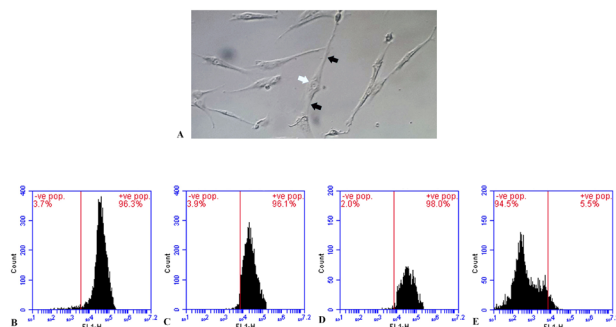


Fig. 1. The identification of rat Bone marrow mesenchymal stem cell (BMMSCs) by microscopy and flowcytometry. The data shows a microscopic image (A) of BMMSCs, taken after 4 days in culture. The cells appear spindle-shaped, with a central cell body (white arrow) and cytoplasmic processes in opposite directions (black arrows). The data also shows flowcytometric identification of BMMSCs, revealing positive expression of specific surface markers: CD44 (B), CD90 (C), and CD105 (D) and negative expression for hemopoietic and endothelial surface marker CD34 (E).

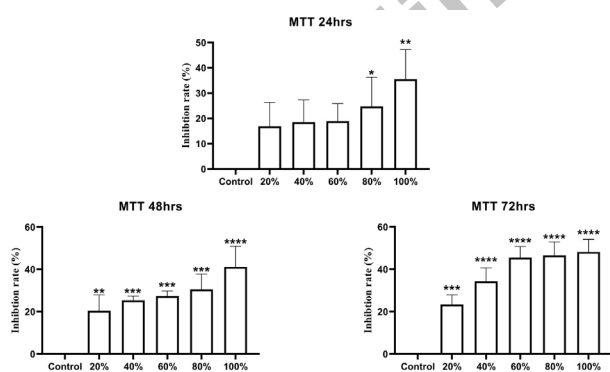


Fig. 2. The inhibitory effect of Bone marrow mesenchymal stem cells-conditioned medium (BMMSCs-CM) on the hepatocellular carcinoma cell line HepG2 by MTT assay. The data shows the inhibition rate (%) of untreated HepG2 cell group (control) and treated HepG2 cell groups with different concentrations of BMMSC-CM (20%-100%) over 24, 48, and 72 h. Values are expressed as mean \pm SD, ($n=3$ /Time group), each concentration group/time was compared to the control group. (* $P<0.05$, ** $P<0.01$, *** $P<0.001$, **** $P<0.0001$).

Effect of BMMSCs-CM on HepG2 cell apoptosis and cell cycle

Flowcytometric detection of apoptosis revealed an increase in the apoptotic % of HepG2 cells after treatment with 100% BMMSCs-CM for 72 h. The apoptotic % of non-treated HepG2 cells was 5.4%, which increased to 26.2% after treatment with 100% BMMSCs-CM for 72 h. The apoptotic % of HepG2 cells treated with BMMSCs-CM was significantly different from that of the non-treated HepG2 cells ($P<0.01$) (Fig. 3). Cell cycle analysis using flowcytometry showed a significant increase in Sub-G1 (5.5% to 17.8%) and G0/G1 (38.3% to 67.23%) phases indicating cell cycle arrest in the G0/G1 phase, and a significant decrease in S (40.1% to 15.87%) and G2/M (18.5% to 1.5%) phases of the HepG2 cell cycle after treatment with 100%BMMSCs-CM for 72 h compared to non-treated HepG2 cells (Fig. 4).

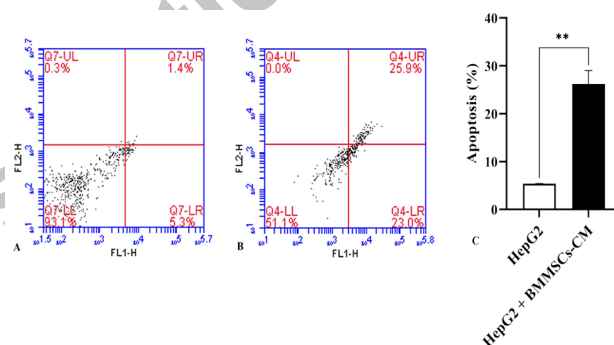


Fig. 3. The apoptotic effect of Bone marrow mesenchymal stem cells-conditioned medium (BMMSCs-CM) on the hepatocellular carcinoma cell line HepG2 using Annexin-Propidium Iodide (PI) stains by flowcytometry. The data shows Annexin-PI measurements of untreated HepG2 cell group (control) (A) and treated HepG2 cell groups with 100% BMMSC-CM for 72 h (B), where the x-axis represents Annexin V-Fluorescein Isothiocyanate (FITC) staining and the y-axis represent PI staining, and the statistical analysis (C). Values are expressed as mean \pm SD, ($n=3$), the treated group (HepG2+BMMSC-CM) was compared to the control group (HepG2). (** $P<0.01$).

Effect of BMMSCs-CM on p53 and Bcl-2 mRNA expression levels in HepG2 cells

p53 and *Bcl-2* mRNA expression levels were evaluated after treating HepG2 cells with 100% BMMSCs-CM for 72 h. The mRNA expression level of *p53* increased significantly in the treated group compared to that of the control group ($P<0.05$), while the mRNA expression level of *Bcl-2* decreased significantly in the treated group compared to that of the control group ($P<0.05$) (Fig. 5).

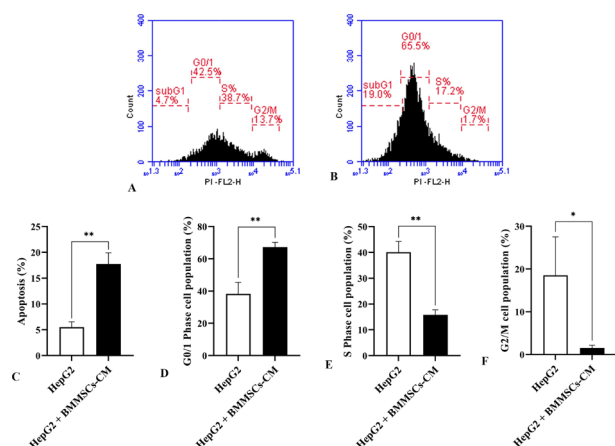


Fig. 4. The impact of bone marrow mesenchymal stem cells-conditioned medium (BMMSCs-CM) on the hepatocellular carcinoma cell line HepG2 cell cycle by flowcytometry. The data shows the cell cycle of untreated HepG2 cell group (control) (A) and treated HepG2 cell groups with 100% BMMSC-CM for 72 h (B). The data shows the statistical analysis for each phase of the cell cycle (SubG1 phase (apoptosis)(C), G0/1 phase (D), S phase (E), and G2/M phase (F). Values are expressed as mean \pm SD, (n=3), the treated group (HepG2=BMMSC-CM) was compared to the control group (HepG2). (* P <0.05, ** P <0.01).

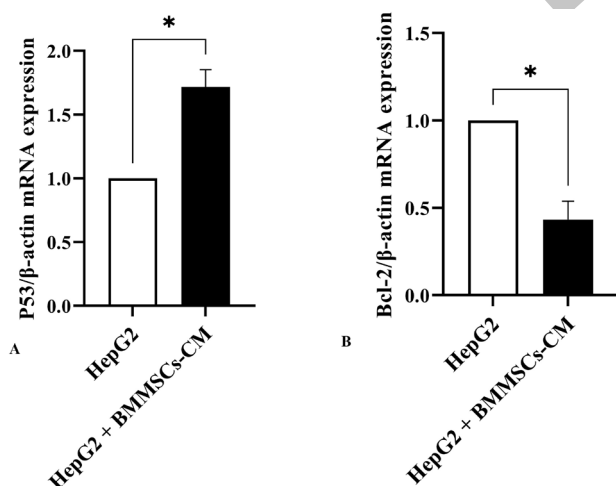


Fig. 5. The influence of bone marrow mesenchymal stem cells-conditioned medium (BMMSCs-CM) on the hepatocellular carcinoma cell line HepG2 mRNA expression of P53 gene (A) and Bcl-2 gene (B) by RT-PCR. The data shows the untreated HepG2 cell group (control) and treated HepG2 cell groups with 100% BMMSC-CM for 72 h. B-actin was used as the house-keeping gene. Values are expressed as mean \pm SD, (n=3), the treated group (HepG2=BMMSC-CM) was compared to the control group (HepG2). (* P <0.05).

Effect of BMMSCs-CM on p53 and Bcl-2 protein levels in HepG2 cells by western blotting

HepG2 cells treated with 100% BMMSCs-CM for 72 h were evaluated by western blotting for p53 and Bcl-2 protein levels. HepG2 cells cultured for 72 h without treatment served as the control group. The results revealed a significant upregulation in p53 protein level in the treated group compared to that of the control group (P < 0.05). However, Bcl-2 protein level was significantly downregulated in the treated group compared to that of the control group (P < 0.01) (Fig. 6).

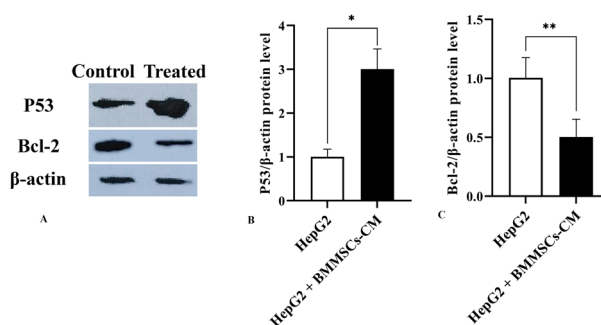


Fig. 6. The effect of bone marrow mesenchymal stem cells-conditioned medium (BMMSCs-CM) on the hepatocellular carcinoma cell line HepG2 protein expression of P53 and Bcl-2 by western blotting. The data shows western blot bands of untreated HepG2 cell group (control), and the treated HepG2 cell group with 100% BMMSC-CM for 72 h for P53 and Bcl-2 protein expression with β-actin as the house keeping protein (A), and the statistical analysis for P53 (B) Bcl-2 (C) proteins expression. Values are expressed as mean \pm SD, (n=3), the treated group (HepG2=BMMSC-CM) was compared to the control group. (* P <0.05, ** P <0.01).

Effect of BMMSCs-CM on p53 and Bcl-2 protein levels in HepG2 cells by flowcytometry

The protein levels of p53 and Bcl-2 were evaluated by flowcytometry after HepG2 cells were treated with 100% BMMSCs-CM for 72 h. HepG2 cells cultured for 72 h without treatment served as the control group. The results revealed a significant upregulation in p53 protein level from 22.87% in the control group to 70.5% in the treated group (P < 0.001). However, Bcl-2 protein level was significantly downregulated from 81.7% in the control group to 19.8% in the treated group (P < 0.001) (Fig. 7).

Effect of BMMSCs-CM on TLR4 concentration in HepG2 cells by ELISA

HepG2 cells were evaluated by ELISA for TLR4 concentration after treatment with 100% BMMSCs-CM for 72 h. HepG2 cells cultured for 72 h without treatment

served as the control group. The results revealed a significant reduction in TLR4 concentration from 21.83 ng/ml in the control group to 6.31 ng/ml in the treated group ($P < 0.05$) (Fig. 8).

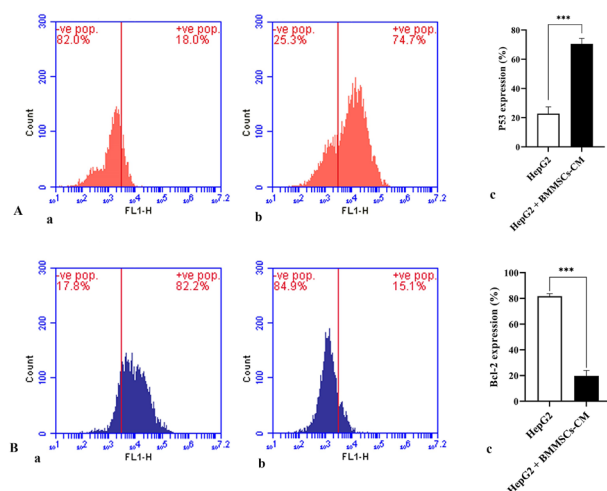


Fig. 7. The effect of bone marrow mesenchymal stem cells-conditioned medium (BMMSCs-CM) on the hepatocellular carcinoma cell line HepG2 protein expression of P53 (A) and Bcl-2 (B) by flow cytometry. The data shows the untreated HepG2 cell group (control), for P53 (Aa) and Bcl-2 (Ba) protein expression, and the statistical analysis for P53 (Ac) Bcl-2 (Bc) proteins expression. Values are expressed as mean \pm SD, (n=3), the treated group (HepG2=BMMSC-CM) was compared to the control group. (* $P < 0.05$, ** $P < 0.01$).

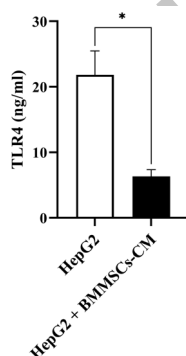


Fig. 8. The influence of bone marrow mesenchymal stem cells-conditioned medium (BMMSCs-CM) on Toll-like receptor 4 (TLR4) concentration in the hepatocellular carcinoma cell line HepG2 by ELISA. The data shows the quantitative values of TLR4 concentration for untreated HepG2 cell group (control) and treated HepG2 cell groups with 100% BMMSC-CM for 72 h. Values are expressed as mean \pm SD, (n=3), the treated group (HepG2=BMMSC-CM) was compared to the control group (HepG2). (* $P < 0.05$).

DISCUSSION

MSCs have been the focus of recent investigations for their antitumorogenic effects. They have been reported by multiple studies to inhibit cancer development, including cases of Lewis' lung carcinoma, B16 melanoma (Maestroni *et al.*, 1999), colon carcinoma (Ohlsson *et al.*, 2003), Kaposi's sarcoma (Khakoo *et al.*, 2006), lymphoma, insulinoma (Lu *et al.*, 2008), breast cancer (Sun *et al.*, 2009), pancreatic cancer (Kidd *et al.*, 2010) and hepatic cancer, specifically HCC (Qiao *et al.*, 2008). Furthermore, it has been proposed that MSCs-CM contain soluble factors that are involved in tumor suppression (Hou *et al.*, 2014; Serhal *et al.*, 2019). In our experiment, we investigated the *in vitro* effect of BMMSCs-CM on HepG2, and it clearly showed that BMMSCs-CM can suppress the proliferation of HepG2.

The CM of BMMSCs was cocultured with HepG2 at different concentrations for up to 72 h. The MTT assay revealed a significant reduction in the viability of HepG2 cells, reaching its lowest when cocultured with 100% BMMSCs-CM for 72 h. These findings matched those of (Hou *et al.*, 2014), but our results were more significant, with lower HepG2 cell viability. Further evaluation of the HepG2 cell cycle in our experiment showed cycle arrest in the G0/G1 phase with inhibition of entry into the S phase. These findings were almost indistinguishable from those of Ramasamy *et al.* (2007), who used MSCs and showed G0/G1 cell cycle arrest, whereas we used BMMSCs-CM instead of the cells themselves. To a similar extent, Khakoo *et al.* (2006) showed that MSCs were capable of suppressing the development of Kaposi's sarcoma via cell-cell interactions. However, the results from our MTT and cell cycle assays indicated that direct contact was not required for BMMSCs to exert their inhibitory effect on HepG2 cells, and that BMMSCs-CM was capable of producing the same suppressive effect.

We further investigated the suppressive effect of BMMSCs-CM on hepG2 cells by flow cytometric analysis of HepG2 cell apoptosis. Our findings revealed significant apoptotic activity of HepG2 cells after treatment with 100% BMMSCs-CM for 72 h. It has been demonstrated that BMMSCs coculture with ascitogenous hepatoma cells (H22) causes a dramatic increase in H22 cell apoptosis (Lu *et al.*, 2008), whereas in this current study, BMMSCs-CM was found to exhibit a similar apoptotic effect on HepG2 cells. The activation of several signaling pathways has been implicated in human hepatocarcinogenesis (Villanueva *et al.*, 2007). Their importance stems from their ability to serve as targets for new therapies (Llovet *et al.*, 2008; Miele *et al.*, 2006). Of these, Notch signaling has been reported to play a critical role in HCC (Villanueva

et al., 2007). Cantarini *et al.* (2006) demonstrated overexpression of Notch 1 in all 15 paired HCC human samples, and the evaluation of 87 resected HCC tumors by Gao *et al.* (2008) revealed upregulation of Notch 1 in 89% of tumor specimens. Furthermore, Notch signaling has been shown to positively regulate cell proliferation in the hepatoma HepG2 cell line (Suwanjune *et al.*, 2008; Wang *et al.*, 2010). However, in a limited number of tumors such as skin and small lung tumors, Notch signaling was antiproliferative rather than oncogenic (Miele *et al.*, 2006). Several mechanisms have been suggested to explain the oncogenic role of Notch signaling. It was reported that Notch signaling influenced both *p53* and *Bcl-2*, where activated Notch 1 has been negatively associated with *p53* transactivation (Kim *et al.*, 2007) and inhibited *p53*-dependant apoptosis (Nair *et al.*, 2003), and Notch 3 depletion allowed the upregulation of *p53* with subsequent suppression of HepG2 cells (Giovannini *et al.*, 2006). On the other hand, activated Notch 1 led to overexpression of *Bcl-2* (Ferreira *et al.*, 2012), and the antiapoptotic effect of activated Notch proteins has been attributed to the induction of *Bcl-2* (MacKenzie *et al.*, 2004). Overall, Notch activation led to downregulation of *p53* and upregulation of *Bcl-2*, causing enhanced cancer cell survival and increased resistance to apoptosis. MSCs have been reported to both upregulate *p53* (Serhal *et al.*, 2019) and downregulate *Bcl-2* (Hou *et al.*, 2014). In the present study, *p53* and *Bcl-2* mRNA and protein expressions were investigated using RT-PCR, flowcytometry, and western blotting, respectively. After treating HepG2 cells with 100% BMMSCs-CM for 72 h, we found significant upregulation of *p53* mRNA and protein expression, as well as significant downregulation of *Bcl-2* mRNA and protein expression in HepG2 cells. These results can explain the suppressive apoptotic activity that was revealed by the MTT assay, apoptosis analysis, and cell cycle analysis exerted by BMMSCs-CM on HepG2 cells. We suggest that these results might have been caused by the influence of soluble factors present in BMMSCs-CM through their potential involvement in Notch signaling inhibition.

Another important signaling mechanism related to notch signaling is the (Toll Like Receptor 4) TLR4/ (Nuclear factor kappa B) NF-kB pathway, in which activated TLR4 directly stimulates NF-kB (Kawai and Akira, 2007), enhancing cancer cells' apoptosis resistance and survival (Naugler and Karin, 2008), but when inhibited, apoptosis is more easily triggered. In addition, NF-kB stimulation has been shown to directly activate Notch 1 signaling and further support cancer development (Yao *et al.*, 2007). Seki and Brenner (2008) reported that mice deficient in TLR4 exhibited a much lower frequency of HCC generation. Furthermore, Yang *et al.* (2015) reported

that TLR4 was associated with HCC through activating NF-kB. These reports collectively indicate that TLR4/NF-kB signaling plays a critical role in hepatocarcinogenesis. It was reported by Li *et al.* (2016) that BMMSCs were able to suppress the TLR4/NF-kB signaling pathway, and in another study, MSCs were found to reduce TLR4 expression in HepG2 cells (Hsiao *et al.*, 2015). In this present study, we found that treating HepG2 cells with 100% BMMSCs-CM for 72 h caused significant TLR4 downregulation in HepG2 cells, which matches the results of previous studies, except we used BMMSCs-CM. These results signify the presence of a role for soluble factors of BMMSCs-CM in TLR4/NF-kB pathway inhibition, rendering cancerous cells less resistant to apoptosis. This aligns with the elevated apoptosis of HepG2 cells by BMMSCs-CM recorded in our current study.

We speculate that the inhibitory effect of BMMSCs-CM on HepG2 cells was possible through the BMMSCs' secretome, possibly via extracellular vesicles such as exosomes (Hassanzadeh *et al.*, 2021) that potentially interfered with the expression of tumorigenic proteins of HepG2 cells through involvement in multiple signaling pathways. However, the precise fraction(s) of BMMSCs-CM that is responsible for the suppressive effect on cancer cells has yet to be defined. Our limitations in financial support and the scarcity of previous literature on BMMSCs' secretome have prevented us from describing the specific portion of the secretome responsible for the anti-tumor effects. Additionally, larger group sizes would have provided us with a more accurate representation. Therefore, future investigations into the BMMSCs' secretome are recommended to specify the exact role of particular fractions of BMMSCs-CM on cancer cells.

CONCLUSIONS

The present study shows that BMMSCs-CM had a direct suppressive effect on HepG2 cell proliferation, observed by a decrease in cell viability, induction of apoptosis and cell cycle arrest with elevated expression of apoptotic genes and reduced expression of antiapoptotic genes through possible involvement in multiple signaling pathways such as TLR4 signaling pathway, making BMMSCs-CM a potent candidate for cancer treatment.

Statement of conflict of interest

The authors have declared no conflict of interest.

REFERENCES

- Abdelkawy, K., El-Haggag, S., Ziada, D., Ebaid, N., El-Magd, M., Elbarbry, F.J.B., and Pharmacotherapy,

2020. The effect of genetic variations on ribavirin pharmacokinetics and treatment response in HCV-4 Egyptian patients receiving sofosbuvir/daclatasvir and ribavirin. *Biomed Pharmacother.*, **121**: 109657. <https://doi.org/10.1016/j.biopha.2019.109657>
- Akimoto, K., Kimura, K., Nagano, M., Takano, S., To'a Salazar, G., Yamashita, T., and Ohneda, O., 2013. Umbilical cord blood-derived mesenchymal stem cells inhibit, but adipose tissue-derived mesenchymal stem cells promote, glioblastoma multiforme proliferation. *Stem Cells Dev.*, **22**: 1370-1386. <https://doi.org/10.1089/scd.2012.0486>
- Alzahrani, F.A., El-Magd, M.A., Abdelfattah-Hassan, A., Saleh, A.A., Saadeldin, I.M., El-Shetry, E.S., Badawy, A.A., and Alkarim, S.J.S.C.I., 2018. Potential effect of exosomes derived from cancer stem cells and MSCs on progression of DEN-induced HCC in rats. *Stem Cell Int.*, **2018**: Article ID 8058979. <https://doi.org/10.1155/2018/8058979>
- Andries, V., Vandepoele, K., Staes, K., Berx, G., Bogaert, P., Van Isterdael, G., Ginneberge, D., Parthoens, E., Vandenbussche, J., and Gevaert, K.J.B.C., 2015. NBPF1, a tumor suppressor candidate in neuroblastoma, exerts growth inhibitory effects by inducing a G1 cell cycle arrest. *BMC cancer*, **15**: 1-25. <https://doi.org/10.1186/s12885-015-1408-5>
- Baharara, J., Namvar, F., Ramezani, T., Mousavi, M., and Mohamad, R.J.M., 2015. Silver nanoparticles biosynthesized using *Achillea biebersteinii* flower extract: Apoptosis induction in MCF-7 cells via caspase activation and regulation of *Bax* and *Bcl-2* gene expression. *Molecules*, **20**: 2693-2706. <https://doi.org/10.3390/molecules20022693>
- Cantarini, M.C., de la Monte, S.M., Pang, M., Tong, M., D'Errico, A., Trevisani, F., and Wands, J.R., 2006. Aspartyl-asparagyl β hydroxylase over-expression in human hepatoma is linked to activation of insulin-like growth factor and notch signaling mechanisms. *Hepatology*, **44**: 446-457. <https://doi.org/10.1002/hep.21272>
- Craig, A.J., Von Felden, J., Garcia-Lezana, T., Sarcognato, S., and Villanueva, A., 2020. Tumour evolution in hepatocellular carcinoma. *Nat. Rev. Gastroenterol. Hepatol.*, **17**: 139-152. <https://doi.org/10.1038/s41575-019-0229-4>
- Di-Santo, S., Yang, Z., Wyler von Ballmoos, M., Voelzmann, J., Diehm, N., Baumgartner, I., and Kalka, C., 2009. Novel cell-free strategy for therapeutic angiogenesis: in vitro generated conditioned medium can replace progenitor cell transplantation. *PLoS One*, **4**: e5643. <https://doi.org/10.1371/journal.pone.0005643>
- Dominici, M., Le Blanc, K., Mueller, I., Slaper-Cortenbach, I., Marini, F., Krause, D., Deans, R., Keating, A., Prockop, D., and Horwitz, E., 2006. Minimal criteria for defining multipotent mesenchymal stromal cells. *Int. Soc. Cell. Ther. Posit. Statement Cytother.*, **8**: 315-317. <https://doi.org/10.1080/14653240600855905>
- El-Magd, M.A., Mohamed, Y., El-Shetry, E.S., Elsayed, S.A., Gazia, M.A., Abdel-Aleem, G.A., Shafik, N.M., Abdo, W.S., El-Desouki, N.I. and Basyony, M.A., 2019. Melatonin maximizes the therapeutic potential of non-preconditioned MSCs in a DEN-induced rat model of HCC. *Biomed. Pharmacoth.*, **114**: 108732. <https://doi.org/10.1016/j.biopha.2019.108732>
- Erices, A., Conget, P., and Minguell, J.J., 2000. Mesenchymal progenitor cells in human umbilical cord blood. *Br. J. Haematol.*, **109**: 235-242. <https://doi.org/10.1046/j.1365-2141.2000.01986.x>
- Ferreira, A.C., Suriano, G., Mendes, N., Gomes, B., Wen, X., Carneiro, F., Seruca, R., and Machado, J.C., 2012. E-cadherin impairment increases cell survival through Notch-dependent upregulation of Bcl-2. *Hum. mol. Genet.*, **21**: 334-343. <https://doi.org/10.1093/hmg/ddr469>
- Fukuchi, Y., Nakajima, H., Sugiyama, D., Hirose, I., Kitamura, T., and Tsuji, K., 2004. Human placenta-derived cells have mesenchymal stem/progenitor cell potential. *Stem Cells*, **22**: 649-658. <https://doi.org/10.1634/stemcells.22-5-649>
- Gao, J., Song, Z., Chen, Y., Xia, L., Wang, J., Fan, R., Du, R., Zhang, F., Hong, L., and Song, J., 2008. Deregulated expression of Notch receptors in human hepatocellular carcinoma. *Dig. Liver Dis.*, **40**: 114-121. <https://doi.org/10.1016/j.dld.2007.08.001>
- Giovannini, C., Lacchini, M., Gramantieri, L., Chieco, P., and Bolondi, L., 2006. Notch3 intracellular domain accumulates in HepG2 cell line. *Anticancer Res.*, **26**: 2123-2127.
- Hassanzadeh, A., Rahman, H.S., Markov, A., Endjun, J.J., Zekiy, A.O., Chartrand, M.S., Beheshtkhou, N., Kouhbanani, M.A.J., Marofi, F. and Nikoo, M., 2021. *Mesenchymal stem/stromal cell-derived exosomes in regenerative medicine and cancer; overview of development, challenges, and opportunities.* **12**: 1-22. <https://doi.org/10.1186/s13287-021-02378-7>
- Hou, L., Wang, X., Zhou, Y., Ma, H., Wang, Z., He, J., Hu, H., Guan, W., and Ma, Y., 2014. Inhibitory effect and mechanism of mesenchymal stem cells on liver cancer cells. *Tumor Biol.*, **35**: 1239-1250. <https://doi.org/10.1007/s13277-013-1165-5>

- Hsiao, C.C., Chen, P.H., Cheng, C.I., Tsai, M.S., Chang, C.Y., Lu, S.C., Hsieh, M.C., Lin, Y.C., Lee, P.H., and Kao, Y.H., 2015. Toll-like receptor-4 is a target for suppression of proliferation and chemoresistance in HepG2 hepatoblastoma cells. *Cancer Lett.*, **368**: 144-152. <https://doi.org/10.1016/j.canlet.2015.08.004>
- Karnoub, A.E., Dash, A.B., Vo, A.P., Sullivan, A., Brooks, M.W., Bell, G.W., Richardson, A.L., Polyak, K., Tubo, R., and Weinberg, R.A., 2007. Mesenchymal stem cells within tumour stroma promote breast cancer metastasis. *Nature*, **449**: 557-563. <https://doi.org/10.1038/nature06188>
- Kawai, T., and Akira, S., 2007. Signaling to NF- κ B by Toll-like receptors. *Trends Mol. Med.*, **13**: 460-469. <https://doi.org/10.1016/j.molmed.2007.09.002>
- Khakoo, A.Y., Pati, S., Anderson, S.A., Reid, W., Elshal, M.F., Rovira, I.I., Nguyen, A.T., Malide, D., Combs, C.A., and Hall, G., 2006. Human mesenchymal stem cells exert potent antitumorigenic effects in a model of Kaposi's sarcoma. *J. exp. Med.*, **203**: 1235-1247. <https://doi.org/10.1084/jem.20051921>
- Kidd, S., Caldwell, L., Dietrich, M., Samudio, I., Spaeth, E.L., Watson, K., Shi, Y., Abbruzzese, J., Konopleva, M., and Andreeff, M.J.C., 2010. Mesenchymal stromal cells alone or expressing interferon- β suppress pancreatic tumors in vivo, an effect countered by anti-inflammatory treatment. *Cytotherapy*, **12**: 615-625. <https://doi.org/10.3109/14653241003631815>
- Kim, S., Chae, G., Lee, J., Park, J., Tak, H., Chung, J.H., Park, T., Ahn, J., and Joe, C.O., 2007. Activated Notch1 interacts with p53 to inhibit its phosphorylation and transactivation. *Cell Death Differ.*, **14**: 982-991. <https://doi.org/10.1038/sj.cdd.4402083>
- Kwon, S.G., Kwon, Y.W., Lee, T.W., Park, G.T., and Kim, J.H., 2018. Recent advances in stem cell therapeutics and tissue engineering strategies. *Biomater. Res.*, **22**: 1-8. <https://doi.org/10.1186/s40824-018-0148-4>
- Li, D., Wang, C., Chi, C., Wang, Y., Zhao, J., Fang, J., and Pan, J., 2016. Bone marrow mesenchymal stem cells inhibit lipopolysaccharide-induced inflammatory reactions in macrophages and endothelial cells. *Mediators Inflamm.*, 2631439: 9 pages. <https://doi.org/10.1155/2016/2631439>
- Livak, K.J., and Schmittgen, T.D.J.M., 2001. Analysis of relative gene expression data using real-time quantitative PCR and the 2- $\Delta\Delta$ CT method. *Methods*, **25**: 402-408. <https://doi.org/10.1006/meth.2001.1262>
- Llovet, J.M., Di Bisceglie, A.M., Bruix, J., Kramer, B.S., Lencioni, R., Zhu, A.X., Sherman, M., Schwartz, M., Lotze, M., and Talwalkar, J., 2008. Design and endpoints of clinical trials in hepatocellular carcinoma. *J. Natl. Cancer Inst.*, **100**: 698-711. <https://doi.org/10.1093/jnci/djn134>
- Llovet, J.M., Kelley, R.K., Villanueva, A., Singal, A.G., Pikarsky, E., Roayaie, S., Lencioni, R., Koike, K., Zucman-Rossi, J., and Finn, R.S., 2021. Hepatocellular carcinoma. *Nat. Rev. Dis. Primers*, **7**: 6-6. <https://doi.org/10.1038/s41572-020-00240-3>
- Lu, Y.R., Yuan, Y., Wang, X.J., Wei, L.L., Chen, Y.N., Cong, C., Li, S.F., Long, D., Tan, W.D., and Mao, Y.Q., 2008. The growth inhibitory effect of mesenchymal stem cells on tumor cells *in vitro* and *in vivo*. *Cancer Biol. Ther.*, **7**: 245-251. <https://doi.org/10.4161/cbt.7.2.5296>
- Lukomska, B., Stanaszek, L., Zuba-Surma, E., Legosz, P., Sarzynska, S., and Drela, K., 2019. Challenges and controversies in human mesenchymal stem cell therapy. *Stem Cells Int.*, <https://doi.org/10.1155/2019/9628536>
- MacKenzie, F., Duriez, P., Wong, F., Nosedá, M., and Karsan, A., 2004. Notch4 inhibits endothelial apoptosis via RBP-J κ -dependent and-independent pathways. *J. Biol. Chem.*, **279**: 11657-11663. <https://doi.org/10.1074/jbc.M312102200>
- Maestroni, G., Hertens, E., Galli, P.J.C., and CMLS, M.L.S., 1999. Factors from nonmacrophage bone marrow stromal cells inhibit Lewis lung carcinoma and B16 melanoma growth in mice. *Cell. Mol. Life Sci.*, **55**: 663-667. <https://doi.org/10.1007/s000180050322>
- Mahfouz, D.H., El-Magd, M.A., Mansour, G.H., Wahab, A.H.A., Abdelhamid, I.A. and Elzayat, E.J.M., 2021. Therapeutic potential of snake venom, l-amino oxidase and sorafenib in hepatocellular carcinoma. *Mol. Cell. Toxicol.*, <https://doi.org/10.1007/s13273-021-00151-8>
- Mansour, G.H., El-Magd, M.A., Mahfouz, D.H., Abdelhamid, I.A., Mohamed, M.F., Ibrahim, N.S., Wahab, A.H.A.A., and Elzayat, E.M.J.B.C., 2021. Bee venom and its active component Melittin synergistically potentiate the anticancer effect of Sorafenib against HepG2 cells. *Bioorg. Chem.*, **116**: 105329. <https://doi.org/10.1016/j.bioorg.2021.105329>
- Miele, L., Miao, H., and Nickoloff, B., 2006. NOTCH signaling as a novel cancer therapeutic target. *Curr. Cancer Drug Targets*, **6**: 313-323. <https://doi.org/10.2174/156800906777441771>

- Mohamed, Y., Basyony, M.A., El-Desouki, N.I., Abdo, W.S., and El-Magd, M.A.J.B., 2019. The potential therapeutic effect for melatonin and mesenchymal stem cells on hepatocellular carcinoma. *BioMedicine*, **9**: <https://doi.org/10.1051/bmrcn/2019090424>
- Nair, P., Somasundaram, K., and Krishna, S., 2003. Activated Notch1 inhibits p53-induced apoptosis and sustains transformation by human papillomavirus type 16 E6 and E7 oncogenes through a PI3K-PKB/Akt-dependent pathway. *J. Virol.*, **77**: 7106-7112. <https://doi.org/10.1128/JVI.77.12.7106-7112.2003>
- Naugler, W.E., and Karin, M., 2008. NF- κ B and cancer identifying targets and mechanisms. *Curr. Opin. Genet. Dev.*, **18**: 19-26. <https://doi.org/10.1016/j.gde.2008.01.020>
- Ohlsson, L.B., Varas, L., Kjellman, C., Edvardsen, K., Lindvall, M.J.E., and pathology, M., 2003. Mesenchymal progenitor cell-mediated inhibition of tumor growth *in vivo* and *in vitro* in gelatin matrix. *Exp. Mol. Pathol.*, **75**: 248-255. <https://doi.org/10.1016/j.yexmp.2003.06.001>
- Qiao, L., Xu, Z., Zhao, T., Zhao, Z., Shi, M., Zhao, R.C., Ye, L., and Zhang, X.J.C.R., 2008. Suppression of tumorigenesis by human mesenchymal stem cells in a hepatoma model. *Cell Res.*, **18**: 500-507. <https://doi.org/10.1038/cr.2008.40>
- Ramasamy, R., Lam, E.W., Soeiro, I., Tisato, V., Bonnet, D., and Dazzi, F., 2007. Mesenchymal stem cells inhibit proliferation and apoptosis of tumor cells: impact on *in vivo* tumor growth. *Leukemia*, **21**: 304-310. <https://doi.org/10.1038/sj.leu.2404489>
- Rashed, W.M., Kandeil, M.A.M., Mahmoud, M.O., and Ezzat, S., 2020. Hepatocellular carcinoma (HCC) in Egypt: A comprehensive overview. *J. Egypt. natl. Cancer Inst.*, **32**: 1-11. <https://doi.org/10.1186/s43046-020-0016-x>
- Secunda, R., Vennila, R., Mohanashankar, A., Rajasundari, M., Jeswanth, S., and Surendran, R., 2015. Isolation, expansion and characterisation of mesenchymal stem cells from human bone marrow, adipose tissue, umbilical cord blood and matrix: A comparative study. *Cytotechnology*, **67**: 793-807. <https://doi.org/10.1007/s10616-014-9718-z>
- Seki, E., and Brenner, D.A., 2008. Toll-like receptors and adaptor molecules in liver disease: Update. *Hepatology*, **48**: 322-335. <https://doi.org/10.1002/hep.22306>
- Selim, N.M., Elgazar, A.A., Abdel-Hamid, N.M., Abu El-Magd, M.R., Yasri, A., El-Hefnawy, H.M., and Sobeh, M.J.A., 2019. Chrysophanol, physcion, hesperidin and curcumin modulate the gene expression of pro-inflammatory mediators induced by lps in hepg2. *In Silico Mol. Stud.*, **8**: 371. <https://doi.org/10.3390/antiox8090371>
- Serhal, R., Saliba, N., Hilal, G., Moussa, M., Hassan, G.S., El Atat, O., and Alaaeddine, N.J.W.J.O.G., 2019. Effect of adipose-derived mesenchymal stem cells on hepatocellular carcinoma: *In vitro* inhibition of carcinogenesis. *World J. Gastroenterol.*, **25**: 567. <https://doi.org/10.3748/wjg.v25.i5.567>
- Sun, B., Roh, K.H., Park, J.R., Lee, S.R., Park, S.B., Jung, J.W., Kang, S.K., Lee, Y.S., and Kang, K.S.J.C., 2009. Therapeutic potential of mesenchymal stromal cells in a mouse breast cancer metastasis model. *Cytotherapy*, **11**: 289-298. <https://doi.org/10.1080/14653240902807026>
- Suwanjune, S., Wongchana, W., and Palaga, T., 2008. Inhibition of gamma-secretase affects proliferation of leukemia and hepatoma cell lines through Notch signaling. *Anti-Cancer Drugs*, **19**: 477-486. <https://doi.org/10.1097/CAD.0b013e3282fc6cdd>
- Tae, S.K., Lee, S.H., Park, J.S., and Im, G.I., 2006. Mesenchymal stem cells for tissue engineering and regenerative medicine. *Biomed. Mater.*, **1**: 63. <https://doi.org/10.1088/1748-6041/1/2/003>
- Villanueva, A., Newell, P., Chiang, D.Y., Friedman, S.L., and Llovet, J.M., 2007. *Genomics and signaling pathways in hepatocellular carcinoma*. Paper presented at: Seminars in liver disease (Copyright© 2007 by Thieme Medical Publishers, Inc., 333 Seventh Avenue, New). <https://doi.org/10.1055/s-2006-960171>
- Villaron, E.M., Almeida, J., López-Holgado, N., Alcoceba, M., Sánchez-Abarca, L.I., Sanchez-Guijo, F.M., Alberca, M., Pérez-Simon, J.A., San Miguel, J.F., and Del Cañizo, M.C., 2004. Mesenchymal stem cells are present in peripheral blood and can engraft after allogeneic hematopoietic stem cell transplantation. *Haematologica*, **89**: 1421-1427.
- Wang, Z., Li, Y., and H Sarkar, F., 2010. Notch signaling proteins: legitimate targets for cancer therapy. *Curr. Protein Peptide Sci.*, **11**: 398-408. <https://doi.org/10.2174/138920310791824039>
- Yang, C., Lei, D., Ouyang, W., Ren, J., Li, H., Hu, J., and Huang, S., 2014. Conditioned media from human adipose tissue-derived mesenchymal stem cells and umbilical cord-derived mesenchymal stem cells efficiently induced the apoptosis and differentiation in human glioma cell lines *in vitro*. *BioMed. Res. Int.*, <https://doi.org/10.1155/2014/109389>
- Yang, J., Li, M., and Zheng, Q.C., 2015. Emerging role

- of Toll-like receptor 4 in hepatocellular carcinoma. *J. Hepatocell. Carcinoma*, **2**: 11. <https://doi.org/10.2147/JHC.S44515>
- Yang, J.D., Hainaut, P., Gores, G.J., Amadou, A., Plymoth, A., and Roberts, L.R., 2019. A global view of hepatocellular carcinoma: Trends, risk, prevention and management. *Nat. Rev. Gastroenterol. Hepatol.*, **16**: 589-604. <https://doi.org/10.1038/s41575-019-0186-y>
- Yao, J., Duan, L., Fan, M., and Wu, X., 2007. γ -secretase inhibitors exerts antitumor activity via down-regulation of Notch and Nuclear factor kappa B in human tongue carcinoma cells. *Oral Dis.*, **13**: 555-563. <https://doi.org/10.1111/j.1601-0825.2006.01334.x>
- Zahran, R., Ghozy, A., Elkholy, S.S., El-Taweel, F., and El-Magd, M., 2020. Combination therapy with melatonin, stem cells and extracellular vesicles is effective in limiting renal ischemia reperfusion injury in a rat model. *Int. J. Urol.*, **27**: 1039-1049. <https://doi.org/10.1111/iju.14345>
- Zuk, P.A., Zhu, M., Ashjian, P., De Ugarte, D.A., Huang, J.I., Mizuno, H., Alfonso, Z.C., Fraser, J.K., Benhaim, P., and Hedrick, M.H., 2002. Human adipose tissue is a source of multipotent stem cells. *Mol. Biol. Cell*, **13**: 4279-4295. <https://doi.org/10.1091/mbc.e02-02-0105>

Online First Article